Hexagonal QAM-Based Two-Way Generalized Code Index Modulation Over Nakagami-m Fading Channels

Fatih Cogen*, Burak Ahmet Ozden ¶§, Erdogan Aydin¶, Nihat Kabaoglu¶
*Turkcell 6GEN. Lab Turkcell Iletisim Hizmetleri Inc., Istanbul, Turkey.
¶Department of Electrical and Electronics Engineering, Istanbul Medeniyet University, Istanbul, Turkey.
§Department of Computer Engineering, Yildiz Technical University, Istanbul, Turkey.
Email: fatih.cogen@turkcell.com.tr, bozden@yildiz.edu.tr, erdogan.aydin, nihat.kabaoglu@medeniyet.edu.tr.

2026 IEEE 23rd Consumer Communications & Networking Conference (CCNC) | 979-8-3315-9673-6/26/$31.00 ©2026 IEEE | DOI: 10.1109/CCNC65079.2026.11366304

***Abstract*—We propose a two-way generalized code index modulation scheme with hexagonal QAM (TW-GCIM-HQAM) over Nakagami-m fading. The design combines GCIM and physical layer network coding with energy-efficient HQAM constellations. Using orthogonal Walsh-Hadamard spreading codes, two users exchange data via a half-duplex relay in two time slots (instead of three in conventional two-way DF). Information is carried by both the HQAM symbols and the indices of the spreading codes on the I/Q branches. We compare the scheme with two-way decode and forward at matched rates and evaluate the average bit error rate via Monte Carlo simulations on Nakagami-m channels for several HQAM constellations. Results show competitive or improved error performance, together with better energy use and time slot efficiency.**

***Index Terms*—Hexagonal QAM, Energy-efficiency, Two-way communication systems, code index modulation, Nakagami-m fading channels**

I. Introduction

Global data demand is surging, driven by online gaming, cloud services, high quality audio and video streaming, low power devices, and the need for connectivity anywhere and anytime. Internet users grew from about 3.9 billion in 2018 to 5.3 billion in 2023, nearly two thirds of the world. Therefore, developing communication systems with high data rate, energy efficiency, and spectral efficiency has become imperative [1]–[3].

Research on energy-efficient communications is accelerating, alongside studies on data rate, latency, and overall efficiency driven by economic, operational, and environmental pressures. In the near future, smart vehicles, drones, medical and wearable devices, sensors, and other IoT endpoints will connect over cellular networks, demanding major capacity growth. Such traffic increases are sustainable only if cellular systems become more organized and both spectrally and energy efficient [4], [5].

Over the last decade, interest in index modulation (IM) has surged. IM encodes information in the indices of resources such as antennas, subcarriers, carriers, time slots, space-time patterns, antenna activation order, modulation type, and spreading codes, so extra bits are conveyed with little or no additional energy. This improves spectral efficiency and reduces hardware cost [6]–[8].

This work was supported by The Scientific and Technological Research Council of Turkey (TUBITAK) through the 1515 Frontier Research and Development Laboratories Support Program under Project 5229901 - 6GEN. Lab: 6G and Artificial Intelligence Laboratory. Also, this work was supported by TUBITAK 1001 (Grant Number: 123E513).

This study uses code-index modulation over spread spectrum (CIM-SS), a competitive and increasingly popular IM variant. CIM-SS builds on direct-sequence spread spectrum (DS-SS): symbols are multiplied by spreading codes to improve robustness to noise and jamming. Unlike plain DS-SS, CIM-SS also maps bits to the spreading code indices, embedding extra data in the signal and achieving higher throughput with the same energy and hardware [1], [2]. Additionally, GCIM generalizes CIM-SS; see [1] for details.

High-order M-ary constellations are widely used in next-generation systems. QAM and PSK are popular for their simplicity, yet they are energy suboptimal. HQAM arranges points on a honeycomb lattice with 60° neighbors, increasing the minimum distance for a given average symbol power and thus improving energy efficiency. Studies show HQAM attains QAM like BER/SER at medium and high SNR with lower average power [9]–[13].

Another key pillar of this study is network coding. In cooperative relaying, spectral efficiency drops because relays and extra time slots are required. Physical layer network coding, also called two way (TW) communication, addresses this with two slots: both users transmit to the relay, the relay XORs the detected bits and broadcasts the result, and each user XORs it with its own bits to recover the partner's data [14]. This reduces time slots and improves spectral efficiency.

We propose TW-GCIM-HQAM, which combines high rate and energy efficient GCIM with energy efficient HQAM and physical layer network coding over Nakagami-m fading channels. Two users exchange data via a half-duplex relay in two time slots. We compare the scheme with two way decode and forward (TW-DF) at equal rate and evaluate average BER through analysis and Monte Carlo simulations on Nakagami-m channels for several HQAM constellations. We adopt the following notation[1].

II. Hexagonal QAM (HQAM) Constellations

Rising demand for energy-efficient, high-rate transmission has renewed interest in HQAM. Compared with conventional QAM and PSK, HQAM lowers peak and average power for a

[1]*Notation:* The following notation is used throughout this paper. *i)* Bold lower/upper case symbols represent vectors/matrices; *ii)* $(\cdot)^H$, $(\cdot)^T$, $\|\cdot\|_F$, $|\cdot|$ and $E[\cdot]$ denote Hermitian, transpose, Frobenius norm, Euclidean norm and expectation operators, respectively, $\Re(.)$ and $\Im(.)$ are the real and imaginary parts of a complex-valued quantity; *iii)* $\binom{\cdot}{\cdot}$ denotes the binomial coefficient.

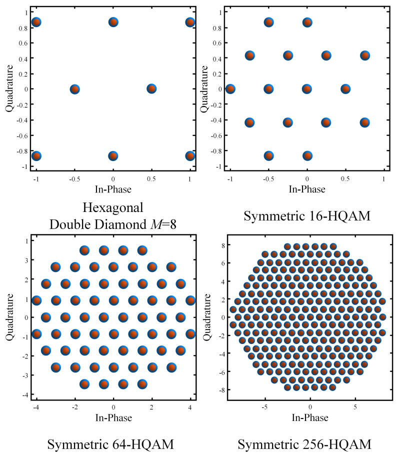

Fig. 1. Various HQAM Constellations

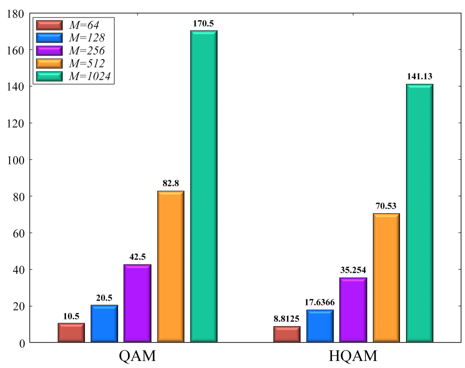

Fig. 2. $P_{average}$ (average power) comparisons of HQAM and QAM when $M = 8, 16, 32$ and 64 [11].

given minimum distance, and recent processing advances have eased its detection complexity. As a result, HQAM is being explored in MIMO, multicarrier, small cell, channel coded, and optical systems.

Fig. 1 shows representative HQAM constellations, and Fig. 3 gives $M = 8$ examples illustrating design diversity. Relative to QAM, HQAM offers higher energy efficiency while maintaining nearly identical BER and SER at moderate to high SNR, which is attractive for power constrained links. Fig. 2 compares QAM and HQAM via minimum Euclidean distance (a proxy for energy efficiency); power is expressed in W per unit squared. See [15] for further details.

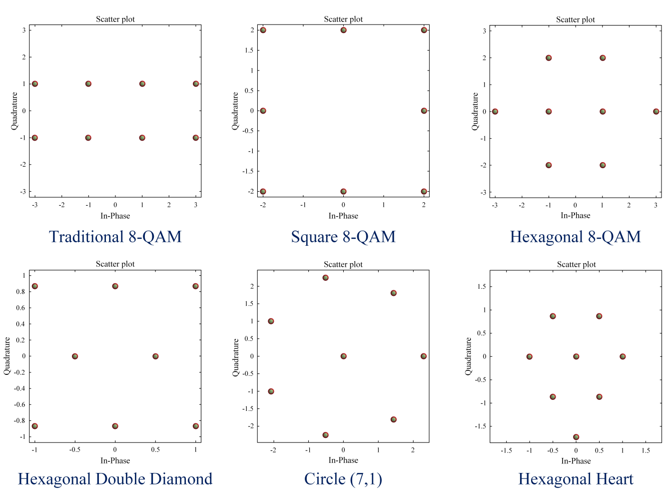

Fig. 3. HQAM Constellations with $M = 8$ [10].

III. System Model

The proposed TW-CIM-HQAM system is shown in Fig. III. Single-antenna sources S_1 and S_2 communicate via a single-antenna relay R. Each source employs N orthogonal Walsh Hadamard spreading codes of length N_c. For S_1 and S_2, the ith codes are $\mathbf{w}_{i_1} = [w_{i_1,1}, \ldots, w_{i_1,N_c}]^T$ and $\mathbf{w}_{i_2} = [w_{i_2,1}, \ldots, w_{i_2,N_c}]^T$, with $i_1, i_2 \in \{1, \ldots, N\}$. The corresponding codebooks are $\mathbf{W}_1 = [\mathbf{w}_1, \ldots, \mathbf{w}_N]$ and $\mathbf{W}_2 = [\mathbf{w}_1, \ldots, \mathbf{w}_N]$, known to S_1, S_2, and R, with $\mathbf{W}_1 \neq \mathbf{W}_2$, so a total of $2N$ codes are used. In-phase (I) and quadrature (Q) branches are used at all nodes to increase data rate, and symbols are HQAM. Overall, the design combines network coding, CIM, and HQAM.

The protocol uses two-way relaying. Two users exchange data via a half-duplex relay R in two time slots thanks to orthogonal spreading; in contrast, conventional TW-DF needs at least three. In slot 1 (multiple access), S_1 and S_2 transmit simultaneously. Relay R despreads the I/Q branches with correlators, applies ML detection, and obtains $\hat{\mathbf{b}}_1^R$ and $\hat{\mathbf{b}}_2^R$. In slot 2 (broadcast), R forms $\mathbf{b}_R = \hat{\mathbf{b}}_1^R \oplus \hat{\mathbf{b}}_2^R$, maps it onto HQAM and the users' spreading codes, and broadcasts over I/Q. Each user despreads, detects, and recovers the partner's bits by XORing the received string with its own.

Considering Fig. III, the information vectors $\mathbf{b}_1$ and $\mathbf{b}_2$ are $\eta \times 1$ binary vectors transmitted within the symbol period T_s. At each user, $\eta = \log_2(M) + 2\log_2(N)$ bits are split into $\log_2(M)$ symbol bits and $2\log_2(N)$ index bits. The $\log_2(M)$ bits select an HQAM symbol, and the $2\log_2(N)$ bits select the spreading code indices for the IQ components. Thus, $\log_2(M)$ bits are carried by the HQAM symbol and $2\log_2(N)$ bits by the code indices of the IQ branches.

In slot 1, after carrier recovery, chip-rate sampling, and digitization, the received I/Q vectors at R are:

$$\mathbf{r}_R^I = x_{1I}\mathbf{w}_{i_{1I}}^1 h_1 + x_{2I}\mathbf{w}_{i_{2I}}^2 h_2 + \mathbf{n}^I \quad (1)$$

$$\mathbf{r}_R^Q = x_{1Q}\mathbf{w}_{i_{1Q}}^1 h_1 + x_{2Q}\mathbf{w}_{i_{2Q}}^2 h_2 + \mathbf{n}^Q, \quad (2)$$

where $x_1 = x_{1I} + jx_{1Q}$, $x_2 = x_{2I} + jx_{2Q}$ and $x_1, x_2 \in \{s_1, s_2, \ldots, s_M\}$ are HQAM symbols. h_1 and h_2 are Nakagami-m fading channel coefficients. $\mathbf{n} \sim \mathbb{C}(0, N_0)$ is a complex Gaussian random variable vector with zero mean and variance $N_0/2$ per dimension. From the $\mathbf{r}_R^I$ and $\mathbf{r}_R^Q$ signals received in R, the spreading code indices of the users are first estimated by taking correlator outputs and selecting the maximum element, since if $i = j$ then $\mathbf{w}_i^T\mathbf{w}_j = 1$ and if $i \neq j$ then $\mathbf{w}_i^T\mathbf{w}_j = 0$. Thus, the indices $\hat{i}_{1I}, \hat{i}_{1Q}, \hat{i}_{2I}$ and $\hat{i}_{2Q}$ are estimated.

The Nakagami-m fading channels are modeled as $h(t) = \sqrt{\sum_{q=1}^{m} |h(t)_{q,R}|^2} + j\sqrt{\sum_{q=1}^{m} |h(t)_{q,I}|^2}$. The samples of $h(t)_{q,R}$ and $h(t)_{q,I}$ are i.i.d. Gaussian with zero mean and variance $\sigma_h^2 = 1/(2m)$, where m is the Nakagami parameter. The envelope and phase PDFs are $f(\theta) = \frac{\Gamma(m)|\sin(2\theta)|^{m-1}}{\Gamma^2(m/2)2^m}$ and $f(\nu) = \frac{2\nu^{2m-1}m^m}{\Gamma(m)}e^{-m\nu^2}$. Here, $\Gamma(m)$ is the Gamma function.

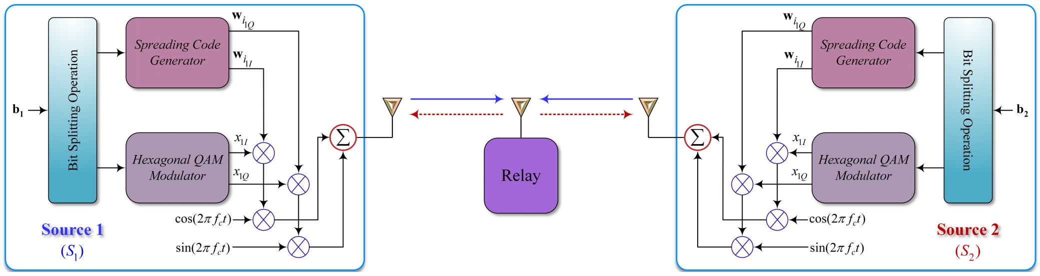

Fig. 4. System model of the TW-CIM-HQAM scheme.

For $m \neq 1$, the phase distribution implied by $f(\theta)$ is not uniform. In R the correlator outputs are obtained as follows:

$$\tilde{\mathbf{r}}^I_{R,S_1} = \mathbf{W}_1^T\mathbf{r}^I_R = \mathbf{W}_1^T\left(x_{1I}\mathbf{w}^1_{i_{1I}}h_1 + x_{2I}\mathbf{w}^2_{i_{2I}}h_2+\mathbf{n}^I\right)$$
$$= \Big[\underbrace{\tilde n^I_1,\dots,\tilde n^I_i}_{i\neq i_{1I}},\underbrace{\left(E_c x_{1I}h_1+\tilde n^I_{i_{1I}}\right)}_{i=i_{1I}},\underbrace{\tilde n^I_{i+1},\dots,\tilde n^I_N}_{i\neq i_{1I}}\Big]^T \quad (3)$$

$$\tilde{\mathbf{r}}^Q_{R,S_1} = \mathbf{W}_1^T\mathbf{r}^Q_R = \mathbf{W}_1^T\left(x_{1Q}\mathbf{w}^1_{i_{1Q}}h_1 + x_{2Q}\mathbf{w}^2_{i_{2Q}}h_2+\mathbf{n}^Q\right)$$
$$= \Big[\underbrace{\tilde n^Q_1,\dots,\tilde n^Q_i}_{i\neq i_{1I}},\underbrace{\left(E_c x_{1Q}h_1+\tilde n^Q_{i_{1Q}}\right)}_{i=i_{1Q}},\underbrace{\tilde n^Q_{i+1},\dots,\tilde n^Q_N}_{i\neq i_{1Q}}\Big]^T \quad (4)$$

$$\tilde{\mathbf{r}}^I_{R,S_2} = \mathbf{W}_2^T\mathbf{r}^I_R = \mathbf{W}_2^T\left(x_{1I}\mathbf{w}^1_{i_{1I}}h_1 + x_{2I}\mathbf{w}^2_{i_{2I}}h_2+\mathbf{n}^I\right)$$
$$= \Big[\underbrace{\tilde n^I_1,\dots,\tilde n^I_i}_{i\neq i_{2I}},\underbrace{\left(E_c x_{2I}h_2+\tilde n^I_{i_{2I}}\right)}_{i=i_{2I}},\underbrace{\tilde n^I_{i+1},\dots,\tilde n^I_N}_{i\neq i_{2I}}\Big]^T \quad (5)$$

$$\tilde{\mathbf{r}}^Q_{R,S_2} = \mathbf{W}_2^T\mathbf{r}^Q_R = \mathbf{W}_2^T\left(x_{1Q}\mathbf{w}^1_{i_{1Q}}h_1 + x_{2Q}\mathbf{w}^2_{i_{2Q}}h_2+\mathbf{n}^Q\right)$$
$$= \Big[\underbrace{\tilde n^Q_1,\dots,\tilde n^Q_i}_{i\neq i_{2I}},\underbrace{\left(E_c x_{2Q}h_2+\tilde n^Q_{i_{2Q}}\right)}_{i=i_{2Q}},\underbrace{\tilde n^Q_{i+1},\dots,\tilde n^Q_N}_{i\neq i_{2Q}}\Big]^T \quad (6)$$

here, E_c is in the form of $E_c = 1/\sqrt{N_c}\sum_{l=1}^{N_c} w^2_{i,l}$. Also, $\tilde n^I_i$ and $\tilde n^Q_i$ are the despreaded noise. The indices $\hat i_{1I}, \hat i_{1Q}, \hat i_{2I}$ and $\hat i_{2Q}$ are the indices of the maximum amplitude elements of $\tilde{\mathbf{r}}^I_{R,S_1}$, $\tilde{\mathbf{r}}^Q_{R,S_1}$, $\tilde{\mathbf{r}}^I_{R,S_2}$, and $\tilde{\mathbf{r}}^Q_{R,S_2}$, and are obtained as follows:

$$\hat i_{1I} = \arg\max_i\left\{\left|\tilde{\mathbf{r}}^I_{R,S_1}\right|\right\},\quad \hat i_{1Q} = \arg\max_i\left\{\left|\tilde{\mathbf{r}}^Q_{R,S_1}\right|\right\}$$
$$\hat i_{2I} = \arg\max_i\left\{\left|\tilde{\mathbf{r}}^I_{R,S_2}\right|\right\},\quad \hat i_{2Q} = \arg\max_i\left\{\left|\tilde{\mathbf{r}}^Q_{R,S_2}\right|\right\}. \quad (7)$$

With the optimum ML detector applied to the $\hat i_{1I}, \hat i_{1Q}, \hat i_{2I}$ and $\hat i_{2Q}$ indexed elements of $\tilde{\mathbf{r}}^I_{R,S_1}$, $\tilde{\mathbf{r}}^Q_{R,S_1}$, $\tilde{\mathbf{r}}^I_{R,S_2}$ and $\tilde{\mathbf{r}}^Q_{R,S_2}$, the symbols $\hat x_1$ and $\hat x_2$ at R are:

$$\hat x^R_1 = \arg\min_{x_1\in\{s_1,s_2,\dots,s_M\}}\left\{\left|\left(\tilde r^{\hat i_{1I}}_{R,S_1} + j\tilde r^{\hat i_{1Q}}_{R,S_1}\right) - E_c x_1 h_1\right|^2\right\},$$
$$= \arg\min_{x_1\in\{s_1,s_2,\dots,s_M\}}\left\{\left|\left(\tilde r^{\hat i_{1I}}_{R,S_1} + j\tilde r^{\hat i_{1Q}}_{R,S_1}\right) - E_c\left(x_{1I}+jx_{1Q}\right)h_1\right|^2\right\},$$

$$\hat x^R_2 = \arg\min_{x_2\in\{s_1,s_2,\dots,s_M\}}\left\{\left|\left(\tilde r^{\hat i_{2I}}_{R,S_2} + j\tilde r^{\hat i_{2Q}}_{R,S_2}\right) - E_c x_2 h_2\right|^2\right\},$$
$$= \arg\min_{x_2\in\{s_1,s_2,\dots,s_M\}}\left\{\left|\left(\tilde r^{\hat i_{2I}}_{R,S_2} + j\tilde r^{\hat i_{2Q}}_{R,S_2}\right) - E_c\left(x_{2I}+jx_{2Q}\right)h_2\right|^2\right\}. \quad (8)$$

Using the indices $\left(\hat i_{1I}, \hat i_{1Q}, \hat i_{2I}, \hat i_{2Q}\right)$ and symbols $\hat x_1, \hat x_2$ obtained in R, we recover the bit strings of S_1 and S_2. The "network coding" is then formed by applying the XOR operation at R as follows:

$$\mathbf{b}_R = \hat{\mathbf{b}}^R_1 \oplus \hat{\mathbf{b}}^R_2. \quad (9)$$

In time slot 2, at R, as in the transmitters of S_1 and S_2, the $\mathbf{b}_R$ bit sequence is split into $\log_2(M)$ and $2\log_2(N)$ sub-vectors. The $\log_2(M)$ bits select $x_R = x_{RI} + x_{RQ}$, and the $2\log_2(N)$ bits select the spreading code for both S_1 and S_2; R then transmits them in IQ-components. Consequently, with $j \in \{1,2\}$, the noisy and faded signal at the j^{th} user for the IQ-components, after perfect carrier detection and sampled at chip rate, is:

$$\mathbf{r}^I_j = x_{RI}\left(\mathbf{w}^1_{i_{1I}} + \mathbf{w}^2_{i_{2I}}\right)h_j + \mathbf{n}^I, \quad (10)$$
$$\mathbf{r}^Q_j = xRQ\left(\mathbf{w}^1_{i_{1Q}} + \mathbf{w}^2_{i_{2Q}}\right)h_j + \mathbf{n}^Q. \quad (11)$$

At each user, as in R, the received signals are passed through correlators and a max selector on the outputs yields the spreading code indices as follows:

$$\hat i_{jI} = \arg\max_i\left\{\left|\Big[\underbrace{\tilde n^I_1,\dots,\tilde n^I_i}_{i\neq i_{jI}},\underbrace{\left(E_c x_{RI}h_j+\tilde n^I_{i_{jI}}\right)}_{i=i_{jI}},\underbrace{\tilde n^I_{i+1},\dots,\tilde n^I_N}_{i\neq i_{jI}}\Big]\right|\right\}$$
$$\hat i_{jQ} = \arg\max_i\left\{\left|\Big[\underbrace{\tilde n^Q_1,\dots,\tilde n^I_i}_{i\neq i_{jQ}},\underbrace{\left(E_c x_{RQ}h_j+\tilde n^Q_{i_{jI}}\right)}_{i=i_{jQ}},\underbrace{\tilde n^Q_{i+1},\dots,\tilde n^Q_N}_{i\neq i_{jQ}}\Big]\right|\right\}. \quad (12)$$

With optimum ML detection on the $\hat i_{jI}$ and $\hat i_{jQ}$ indexed elements of $\tilde{\mathbf{r}}^I_j$ and $\tilde{\mathbf{r}}^Q_j$, the user symbols are obtained as:

$$\hat x_j = \arg\min_{x_j\in\{s_1,s_2,\dots,M\}}\left\{\left|\left(\tilde r^{\hat i_{jI}}_j + j\tilde r^{\hat i_{jI}}_j\right) - E_c x_j h_j\right|^2\right\}. \quad (13)$$

Using $\hat i_{jI}, \hat i_{jQ}$ and $\hat x_j$ indices and symbols, users obtain the estimated bit sequence $\hat{\mathbf{b}}^j_R$ with bitwise backmapping. As a result, each user decides the other user's information as follows:

$$\hat{\mathbf{b}}_2 = \hat{\mathbf{b}}^1_R \oplus \mathbf{b}_1 \quad \hat{\mathbf{b}}_1 = \hat{\mathbf{b}}^2_R \oplus \mathbf{b}_2. \quad (14)$$

IV. Simulation Results and Discussion

In this section, we present simulation results for the proposed TW-CIM system with QAM and HQAM over Nakagami-m fading. Symbols at R, S_1, and S_2 are detected by optimum ML, and spreading code indices by correlators. Average BER is obtained via Monte Carlo. Here, $\mathrm{SNR(dB)}$ is $\mathrm{SNR(dB)} = 10\log_{10}(E_s/N_0)$, where $E_s = \sum_{l=1}^{N_c}\left(\frac{w_{i,k}}{\sqrt{N_c}}\right)^2$ is the average symbol energy. The spreading codes are normalized with $\sqrt{N_c}$ so that the transmission energy remains constant.

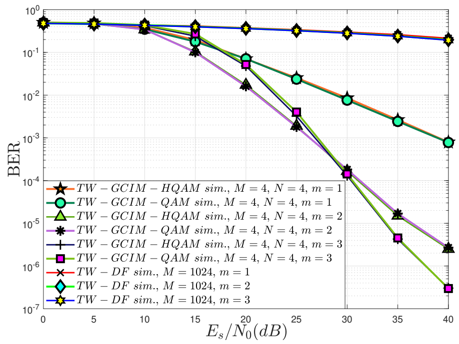

Fig. 5. Performance comparisons of the TW-GCIM-HQAM/QAM and TW-DF systems for $m = 1, 2, 3$ and $\eta = 10$ bits.

Fig. 5 compares TW-GCIM-HQAM/QAM with conventional TW-DF for various Nakagami-m values. TW-GCIM transmits 10 bits per symbol (2 via the modulated symbol and 8 via code indices), whereas TW-DF carries 10 bits solely in the symbol. For $M = 4$, HQAM and QAM give similar BER. At $\mathrm{SNR} = 15$ dB and $\eta = 10$, TW-GCIM outperforms TW-DF by > 25 dB for $m = 1$, about 30 dB for $m = 2$, and about 20 dB for $m = 3$. The advantage is larger at higher SNR.

Fig. 6 compares TW-CIM for $M \in \{8, 16\}$ and $N = 4$ over Nakagami-m fading. In panels (a) and (b), 3 bits are carried by the modulated symbol and 8 by the spreading code indices. Across all cases, TW-CIM-HQAM achieves nearly the same BER as TW-CIM-QAM while using less energy[2].

V. Conclusion

In this study, a new energy-efficient and high data-rated communication technique named TW-GCIM-HQAM is proposed for Nakagami-m channels by combining GCIM technique, energy-efficient HQAM technique and network coding structure, which are promising for next generation communication techniques. The proposed new technique consumes less energy due to the nature of HQAM and is more advantageous in terms of symbol seperation at low energies. With computer simulation results, it has been shown that the proposed TW-GCIM-HQAM system exhibits similar SNR performances in Nakagami-m channels compared to same system using QAM, and also consumes less transmission energy.

References

[1] F. Cogen, E. Aydin, N. Kabaoglu, E. Basar, and H. Ilhan, "Generalized code index modulation and spatial modulation for high rate and energy-efficient MIMO systems on rayleigh block-fading channel," *IEEE Syst. J.*, vol. 15, no. 1, pp. 538–545, 2021.

[2]If all of the figures are examined carefully, it can be understood that TW-CIM-HQAM systems show almost the same BER performances as TW-CIM-QAM systems, while consuming less energy.

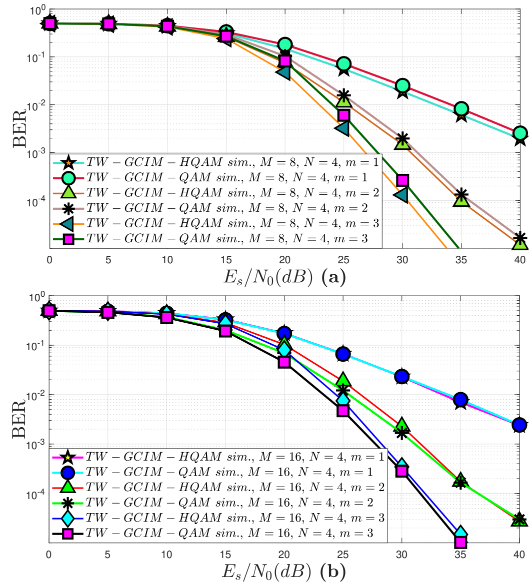

Fig. 6. Performance comparisons of the TW-GCIM-HQAM and TW-GCIM-QAM systems for $m = 1, 2, 3$ and $\eta = 11, 12$ bits.

[2] E. Aydin, F. Cogen, and E. Basar, "Code-index modulation aided quadrature spatial modulation for high-rate MIMO systems," *IEEE Trans. Veh. Technol.*, vol. 68, no. 10, pp. 10 257–10 261, 2019.

[3] Cisco, "Cisco Annual Internet Report (2018–2023) White Paper (March 2020 Update)," pp. 1–37, 2020.

[4] S. Buzzi, I. Chih-Lin, T. E. Klein, H. V. Poor, C. Yang, and A. Zappone, "A survey of energy-efficient techniques for 5G networks and challenges ahead," *IEEE IEEE J. Sel. Areas Commun.*, vol. 34, no. 4, pp. 697–709, apr 2016.

[5] P. Gandotra and R. K. Jha, "A survey on green communication and security challenges in 5G wireless communication networks," *J. Netw. Comput. Appl.*, vol. 96, pp. 39–61, Oct. 2017.

[6] B. A. Ozden and E. Aydin, "Antenna selection for receive spatial modulation system empowered by reconfigurable intelligent surface," *IEEE Trans. Veh. Technol.*, vol. 74, no. 1, pp. 1169–1179, 2025.

[7] E. Basar, M. Wen, R. Mesleh, M. Di Renzo, Y. Xiao, and H. Haas, "Index modulation techniques for next-generation wireless networks," *IEEE Access*, vol. 5, pp. 16 693–16 746, Aug. 2017.

[8] M. Wen, X. Cheng, and L. Yang, *Index Modulation for 5G Wireless Communications*, ser. Wireless Networks. Cham: Springer International Publishing, 2017.

[9] F. Cogen and E. Aydin, "Hexagonal quadrature amplitude modulation aided spatial modulation." in *2019 11th Int. Conf. on Elect. and Electron. Eng. (ELECO)*. IEEE, November 2019.

[10] ——, "Performance analysis of Hexagonal QAM constellations on quadrature spatial modulation with perfect and imperfect channel estimation," *Phys. Commun.*, vol. 47, p. 101379, aug 2021.

[11] E. Aydin, "A new hexagonal quadrature amplitude modulation aided media-based modulation," *Int. J. Commun. Syst.*, vol. 34, no. 17, p. e4994, 2021.

[12] B. A. Ozden, F. Cogen, and E. Aydin, "Mirror activation pattern selection for energy efficient hexagonal qam aided media-based modulation," *Trans. Emerging Telecommun. Technol.*, vol. 34, no. 7, p. e4795, 2023. [Online]. Available: https://onlinelibrary.wiley.com/doi/abs/10.1002/ett.4795

[13] F. Cogen, B. A. Ozden, and E. Aydin, "Ris-assisted hexagonal receive qsm technique with perfect and imperfect channel estimation," in *Proc. 2024 6th Int. Conf. Commun., Signal Process., Appl. (ICCSPA)*, 2024, pp. 1–5.

[14] E. Aydin and F. Cogen, "Two-way code index modulation," in *2019 27th Signal Process. and Commun. Appl. Conf. (SIU)*. IEEE, Apr. 2019, pp. 1–4.

[15] C. D. Murphy, "High-order optimum hexagonal constellations," in *11th IEEE Int. Symp. on Pers. Indoor and Mobile Radio Commun. PIMRC 2000. Proceedings (Cat. No. 00TH8525)*, vol. 1. IEEE, 2000, pp. 143–146.